DOI: 10.1002/ejic.200900470

A Macrocyclic Bistriazene and its Complexes with Divalent Metal Ions

Johannes Beck,*[a] Manfredo Hörner,*[b] and Gertrud Dittmann[a]

Keywords: Triazenido complexes / Macrocyclic ligands / Nickel / Cobalt / Magnetic properties

The diazotisation of 2,2′-diaminotolane with one equivalent of HNO_2 yields the macrocyclic bis(tolanetriazene) (tolaneN$_3$H)$_2$ in moderate yield. As shown by the crystal structure determination, the molecule is essentially planar. After deprotonation, the central cavity is suitable for complexation of transition metal ions. In pyridine solution, the anion (tolaneN$_3$)$_2^{2-}$ is formed, which reacts with the acetates of Co^{2+} and Ni^{2+} to the dark red coloured complexes [M((tolaneN$_3$)$_2$)(py)$_2$]. The metal ions are located in the centre of the macrocycles, coordinated by four N atoms of the two triazenide groups. Two pyridine ligands occupy the axial positions, giving the central atoms a distorted octahedral coordination environment. In the temperature range between 30 and 300 K, both complexes show the expected magnetic properties of magnetically isolated ions with nearly fulfilled Curie behaviour and $\mu_{eff} = 3.40$ for Ni^{II} and 5.19 for Co^{II}, which is in the high spin state.

Introduction

Triazenes are a class of compounds based on the characteristic functional group of three catenated nitrogen atoms, R–N=N–N(H)–R, which exhibit a remarkable broad variety of properties and uses. They have gained application as antitumor drugs (dacarbazine, temozolomide),[1] as buildings blocks in different kinds of organic syntheses[2] like the cyclisation of ethynylphenyl-triazenes to indazole and cinnoline heterocycles.[3] 1,3-Di-substituted triazenes are N–H acidic. Strong bases allow for the deprotonation to the triazenide(1–) ions, which are versatile ligands toward all kinds of metal ions. Different modes of complexation are known. In the majority of the structurally characterized complexes, the bent N_3 group acts via the two outer N atoms as a chelating ligand towards one metal ion making up a four membered chelate ring, but monodentate and μ_2-briging ligation is also known. Complexes have for example been prepared with alkali ions,[4] thallium(I),[5] alkaline earth ions,[6] group 14 metals,[7] and noble metals like Cu^{I} [8] or Pt^{IV}.[9]

The reaction of diazonium salts $R–N{\equiv}N^+ X^-$ with amines $R–NH_2$ is the classical and convenient route to triazenes. An aromatic amine carrying two amino groups can be transferred into the monodiazonium salt by the reaction with only one equivalent of HNO_2. If the amine and the diazonium group are in a suitable orientation one can expect on rising up the pH of the acidic diazonium salt solution an intermolecular ring closure reaction leading to a macrocyclic bistriazenide. The only report in the literature on this kind of reaction is the supposed synthesis of **1**, carried out with 2,2′-diaminobiphenyl. Based on spectroscopic data the synthesis of the macrocyclic bis(biphenyltriazene) **1** bearing two biphenyl groups linked by two triazene units besides several other products has been claimed (Figure 1).[10]

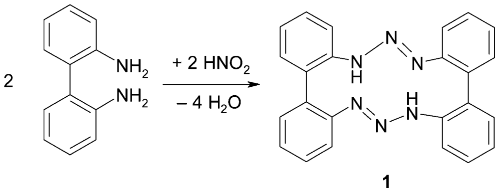

Figure 1. Supposed synthesis of 9,20-dihydrotetrabenzo[*d*,*f*,*k*,*m*]-[1,2,3,8,9,10]hexaazacyclotetradecine (**1**).[10]

Cyclic molecules with this kind of structure are unexplored but interesting, since they are in principle bifunctional. Due to the polar N–H bonds and the positively polarized H atoms anion binding should be possible. In the deprotonated state they can act as ligands towards cations inside the central cavity.

This work forms part of our studies on metal complexes of bis(triazenides).[11] Metal complexes of macrocyles containing trizenido groups as part of a large ring have not yet been reported. We achieved the synthesis of the first structurally characterized macrocyclic bistriazene and the first metal complexes thereof.

---

[a] Institute for Inorganic Chemistry, University of Bonn,
Gerhard-Domagk-Str. 1, 53121 Bonn, Germany
Fax: +49-228-73-5660
E-mail: j.beck@uni-bonn.de
[b] Universidade Federal de Santa Maria, Departamento de Química,
Caixa Postal 5031, 97.105-970 Santa Maria, RS, Brazil
Fax: +55-3220-8031
E-mail: hoerner@smail.ufsm.br

Results and Discussion

In order to explore the properties of **1** we tried to repeat the described[10b] procedure but all our attempts to obtain **1** were unsuccessful. Separation of the reaction mixtures by flash chromatography gave only carbazole. It is a common feature of diaryltriazenes that the angulate $N_3(H)$ group is in plane with the adjacent benzene rings giving the diaryltriazene unit Ph–N(H)NN–Ph an almost planar shape. Thereby a maximum of π orbital overlap and resonance between the aromatic rings and the $N_3(H)$ group is achieved. Simply building a mechanical model of molecule **1** shows that planarity is not possible without bringing the two hydrogen atoms in a too close contact to the N atoms of the opposite triazene unit. All conformations of **1** without falling below the van der Waals limit for neighbouring atoms are strongly tilted and high internal strain is present. So the existence of **1** remains doubtful.

These problems can be overcome by inserting spacer groups into the bonds between the phenyl rings. Ethynyl groups seem to be suitable, since they preserve the linearity and shift the two triazene groups by about 2.6 Å away from each other. Thus replacing the biphenyl moiety Ph–Ph by a tolane group (Ph–C≡C–Ph) results in the molecular structure $(\text{tolaneN}_3\text{H})_2$ **2** (Figure 2). The mechanical molecular model shows that this molecule allows for complete coplanarity of all atoms without any intramolecular strain. Moreover, the two distances of the outer N atoms of one triazene group to the opposite N atoms of the second triazene group amount to about 4.5 Å, which corresponds well with twice the lengths of transition metal–nitrogen single bonds. In the deprotonated state, $(\text{tolaneN}_3)_2^{2-}$ can therefore be expected to act as a macrocyclic ligand able to incorporate transition metal ions in the central cavity.

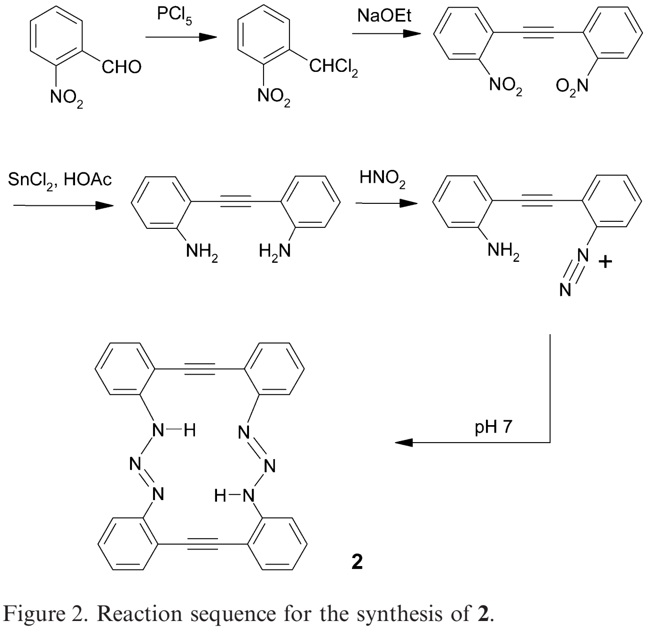

Figure 2. Reaction sequence for the synthesis of **2**.

A reaction sequence was set up for the synthesis of **2** starting from commercially available 2-nitrobenzaldehyde, which was converted to 2-nitrobenzal chloride with PCl_5 in toluene followed by steam distillation.[12] 2,2′-Dinitrotolane was obtained from 2-nitrobenzal chloride and sodium ethoxide in ethanol.[13] The reduction of 2,2′-dinitrotolane to 2,2′-diaminotolane was performed by the use of $SnCl_2$ in acetic acid and ultrasonic irradiation.[14] The physical and spectroscopic parameters of these three compounds were in line with the literature data.

In the last and decisive step, 2,2′-diaminotolane was transferred into the monodiazonium salt by one equivalent of $NaNO_2$/HCl. Slowly raising the pH of the strongly acidic solution to the neutral range afforded a dark yellow precipitation, from which **2** could be isolated by flash chromatography. The yields of **2** were generally low and did never exceed 11% in the final step. The low yield is perspicuous since the statistical reaction favours oligomerisation rather than the desired ring closure.

2 is obtained as a yellow compound crystallizing in the form of fine needles. The thermal stability is high with a decomposition point above 280 °C. Some samples from the different runs, however, showed explosive behaviour when heated up to this temperature. **2** has a rather low solubility in common solvents. Reasonable concentrations were achieved with THF and DMSO. **2** is well soluble in basic solvents such as pyridine where deprotonation occurs accompanied by the development of a deep orange colour. Crystal growth was performed by dissolving **2** in ethanol in the presence of a just sufficient amount of NaOEt to achieve a clear orange solution. Leaving this solution exposed to air causes slow hydrolysis of the ethylate and **2** recrystallized within two days in the form of transparent yellow needles.

The crystal structure is made of almost planar, only slightly ondulated molecules (Figure 3). The largest deviation from the best plane through all 34 non-hydrogen atoms is observed for N(1) with only 0.160 Å. The molecule has a crystallographic inversion centre in its midpoint. However, the higher point symmetry D_{2h} is almost fulfilled. The length of the ethynyl bridge C(1)–C(2) 1.197 Å is in the expected range for triple bonds, the angles at C(1) and C(2) deviate less than 1.3° from linearity. In the protonated form, triazenes normally show a distinct N–N bond lengths separation into one short and one long bond, corresponding to a double and a single bond according to the formula R–N=N–N(H)–R. A retrieval in the Cambridge Structural Database on 26 diaryltriazenes showed the typical values to be 1.26 and 1.34 Å.[15]

This is not the case for the structure of **2**. Here both N–N distances are equal (1.30 Å). Residual electron density was found at both N atoms N(1) and N(3) and had to be refined as two half-occupied hydrogen atoms. Due to the centre of symmetry in the midpoint of the molecule all four N atoms are attched to a half-occupied H atom. An explanation for this unusal behaviour may be assuming that the molecules are disordered in the crystal. The result of a rotation around each of the crystallographically not present

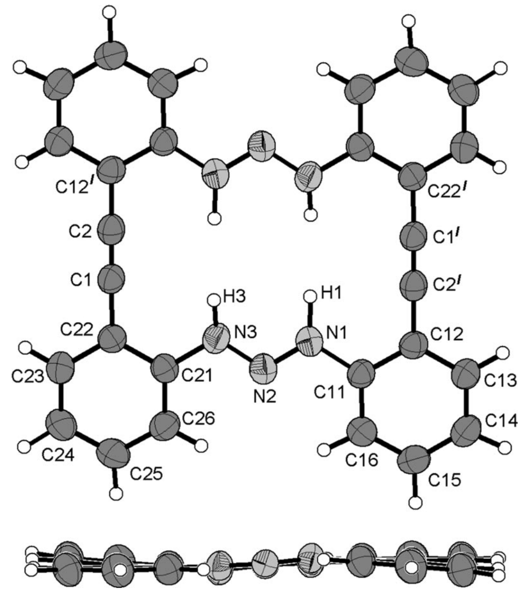

Figure 3. The structure of **2** in a view perpendicular to the molecular plane (top) and parallel to the plane in the direction of the highest deviation from planarity (bottom). Displacement ellipsoids are scaled to enclose a probability density of 50%. The hydrogen atoms H(1) and H(3) each have occupation factors of 0.5.

twofold symmetry axes in the plane of the molecule is the coincidence of all atoms but also the transfer of the hydrogen atom of an odered triazene from N_α to N_γ. Only the H atoms in the inner cavity would be affected by this rotation. Assuming this disorder therefore seems perspicuous. Another possibility is dynamic disorder of the hydrogen atoms. Investigations with solid state NMR spectroscopy are presently in work.

In the crystal, the molecules are arranged in oblique stacks running along the crystallographic *a* axis (Figure 4). Two differently oriented stacks are present in the structure generating a herringbone pattern. The planes of the individual molecules are separated by about 3.2 Å.

In the deprotonated form, the macrocyclic triazenediide $(tolaneN_3)_2^{2-}$ is able to form metal complexes with divalent transition metals. The reaction can simply be performed by dissolving the acetates of Co^{2+} and Ni^{2+} together with **2** in pyridine. The metal complexes $[M((tolaneN_3)_2)(py)_2]\cdot 2py$ [M = Co^{2+} (**3**·2py) and M = Ni^{2+} (**4**·2py)] precipitate out of the solution as dark red crystals. The metal complexes with divalent Co and Ni are crystallographically isotypic. The metal ions are located in inversion centres in the midpoint of the cavity of the macrocyclic ligand (Figure 5). The metal atoms have a distorted octahedral coordination environment and are coordinated to the N_α and N_γ atoms of two triazenide groups in the equatorial plane and two N atoms of pyridine molecules in the axial positions. The Co–N bonds to the N atoms of the axial pyridine ligands amount 2.14 Å, to the triazenide N atoms averaged 2.21 Å. For M = Ni the respective values are 2.08 and 2.18 Å. The M–N(pyridine) bonds are in the usual range, as found for example in the Co^{II} diphenyltriazenido complex $[Co(PhN_3Ph)_2(py)_2]$ (2.19 Å).[16] Here, the M–N(triazenide) bonds are markedly shorter (2.07, 2.17 Å). The same holds for the Ni complex **4**·2py. In the comparable triazenido complex $(PPh_4)[Ni(PhN_3Ph)_3]$ Ni···N distances were found between 2.07 and 2.11 A.[17] The elongated M–N bonds are caused by the rigidity of the structure of the macrocyclic ligand, which determines the lengths of the M–N bonds. The coordination polyhedra are strongly distorted since the two triazenide groups act as chelating ligands making up four-membered strained chelate rings. The N–M–N angles

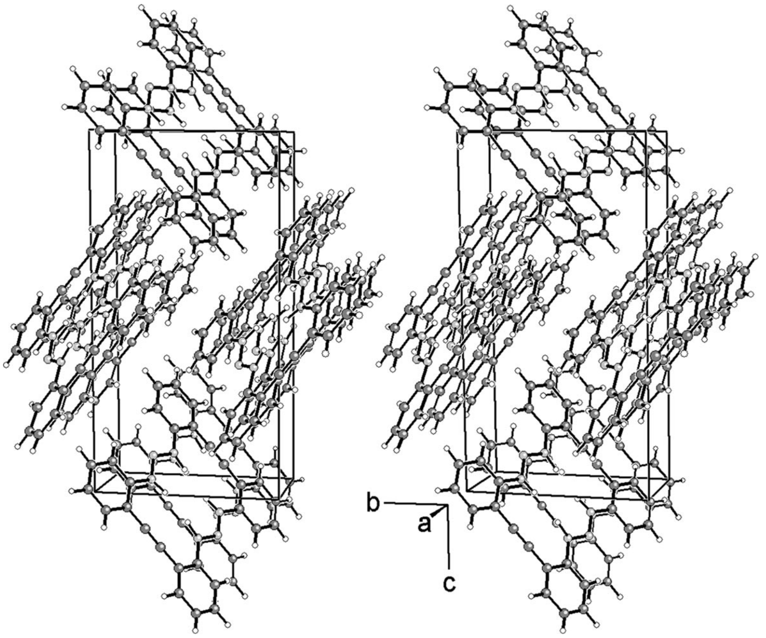

Figure 4. The unit cell of **2** in a stereoscopic view along the crystallographic *a* axis.

within the equatorial planes amount 58° and 122° for M = Co and 59° and 121° for M = Ni. The complexation of the cations does not disturb the planarity of the ligand. The largest deviation of a C or N atom from the best plane through all ligand atoms does not exceed 0.175 Å in the complexes and is not significantly higher in comparison with the protonated state.

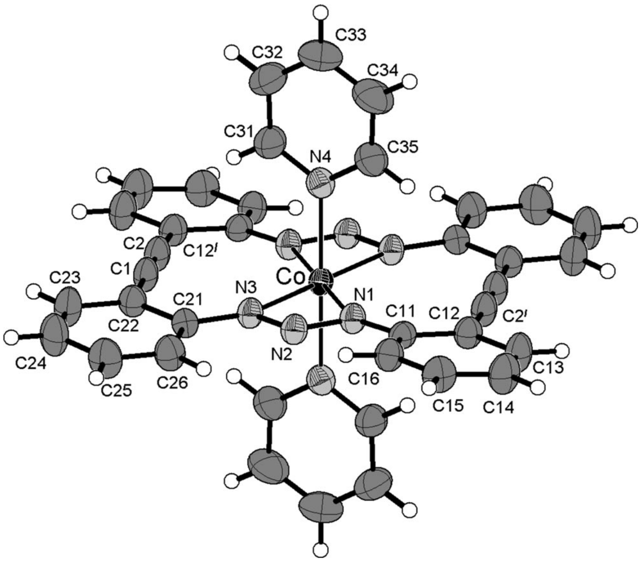

Figure 5. The structure of the complex [Co((tolaneN$_3$)$_2$)(py)$_2$] in the structure of **3**·2py. Displacement ellipsoids are scaled to enclose a probability density of 50%. Symmetry operation: $I = -x + 1/2, -y + 1/2, -z + 1$.

For a magnetically dilute Co^{II} ion in the high-spin state ($S = 3/2$) one expects as a result of spin and first-order orbital contributions μ_{eff} values in the range between 4.3 and 5.2, well above the spin-only value of 3.87 B.M. For dilute Ni^{II} ($S = 1$), these contributions are generally smaller and magnetic moments between 2.8 and 3.5, closer to the spin only value of 2.83 B.M. are observed.[18] Figure 6 shows the inverse molar magnetic susceptibilities of both complexes as a function of the temperature. In the complete registered temperature region between 30 and 300 K, the susceptibility data allow for a linear fit, indicating Curie–Weiss behaviour. Extrapolation to $\chi^{-1} = 0$ gives relatively small Weiss constants of –9.5 K for **3** and –8.7 K for **4**. The magnetic moments are μ_{eff} = 5.19 B.M. for **3** and 3.40 B.M. for **4**. The observed magnetic moments are within the expected range for isolated Co^{II} and Ni^{II} ions and show Co^{II} to be in the high spin state. Apparently, (tolaneN$_3$)$_2$$^{2-}$ is not a strong ligand. This may be caused by the long M–N bonds, caused by the rigidity of the ligand system.

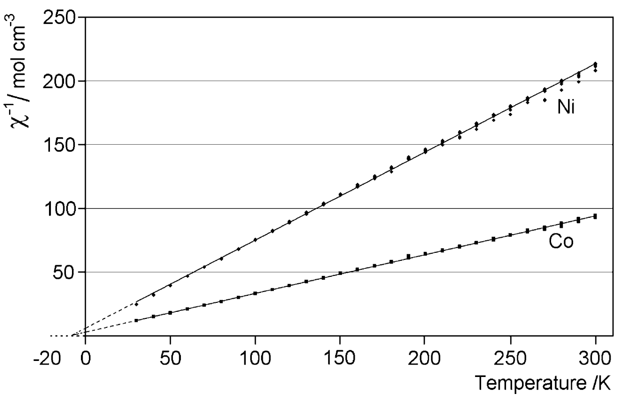

Figure 6. The reciprocal susceptibility $\chi_{mol}{}^{-1}$ for the complexes [Co((tolaneN$_3$)$_2$)(py)$_2$] (**3**) and [Ni((tolaneN$_3$)$_2$)(py)$_2$]·2py (**4**·2py) as a function of the temperature. A linear fit is applied to the χ^{-1} data giving a Curie–Weiss constant of –9.5 K for the Co complex and –8.7 K for the nickel complex.

Conclusions

The intermolecular diazo coupling reaction of 2-diazo-2′-aminotolane yields the macrocyclic bis(tolanetriazene) (tolaneN$_3$H)$_2$, which represents the first structurally characterized triazene with the diazoamino –N=N–N(H)– group as part of ring. The almost planar and D_{2h} symmetric molecule can be deprotonated twice and transferred into the dianion (tolaneN$_3$)$_2$$^{2-}$. The size of the inner cavity of this anion is suitable for the complexation of divalent transition metal cations such as Co^{2+} and Ni^{2+}, which gain an octahedral coordination environment by two additional pyridine ligands in the axial positions. The rigidity of the ring will allow this form of complexation for only such metal ions with a suitable radius to fit into the cavity. The molecular shape of **2** is closely related to the macrocyclic cyclobis(biindolylidyne), which exhibits remarkable anion binding properties.[19] The anion binding capabilities of the bistriazene macrocyclus **2** via X$^-$···H–N bonds and the structures of metal complexes of metal ions with small and large ionic radii are currently under investigation.

Experimental Section

Reagents and Procedures: 2-Nitrobenzaldehyde, phosphorus pentachloride, sodium ethoxide solution and stannous chloride were commercial products (Aldrich Chemical Co.) and used as received. NMR spectra were recorded with a Bruker DPX-300 instrument.

Elemental analyses were carried out with an Elementar Vario microanalyzer. Infrared spectra were recorded using a Bruker IFS-100 instrument with samples embedded in KBr disks, Raman spectra using a Bruker FT Raman spectrometer RFS100 (Nd:YAG laser, 1064 nm, backscattering mode). ESI-TOF mass spectra were recorded with a Bruker Daltonik micrOTOF-Q spectrometer (CH$_3$CN, calibration by sodium formate).

Caution: The thermal decomposition of **2** was observed to be vigorous and explosive. Care must be taken when **2** is exposed to elevated temperatures.

12,13,25,26-Tetradehydro-5,18-dihydrotetrabenzo[*d*,*h*,*m*,*q*]-[1,2,3,10,11,12]hexaazacyclooctadecine (2): In a typical experiment, 3.12 g (15 mmol) 2,2′-diaminotolane[13] was suspended in 80 mL of 6 N hydrochloric acid. The slurry was cooled to 0 °C and a solution o 1.03 g (15 mmol) NaNO$_2$ in water was added dropwise. The temperature was kept below 5 °C during this process. The reaction mixture was agitated for 30 min. A concentrated, cold solution of sodium acetate was then added in small portions until pH 7 was reached. The solution was filtered and the brownish residue was dissolved in THF and chromatographized on silica with THF/hexanes, 1:1 as eluent. The intense yellow fraction was separated. Removal of the solvent left a yellow powder made up of fine crystal needles. Yield in different runs 0.18 g to 0.36 g (5 to 11% of theory); m.p. 280–283 °C with decomposition (see safety comment above). $C_{28}H_{18}N_6$ (438.49): calcd. C 76.7, H 4.1, N 19.2; found C 73.4, H 4.0, N 17.7. ^1H NMR (300 MHz, [D_8]THF, 293 K): δ = 11.3 (s, 1 H, N-H) 6.9–7.7 (m, 8 H, C_{arom}-H) ppm. ^{13}C NMR: δ = 89.0, 95.5 (C≡C), 110.6, 115.4, 119.4, 120.6, 124.3, 128.8, 130.8, 131.2, 132.6, 133.3, 143.8, 152.3 ppm. IR (KBr): $\tilde{\nu}$ = 3262 (s) (N–H), 3050 (w), 3030 (w) (C–H), 2219 (w) (C≡C), 1601 (w), 1579 (s), 1509 (s), 1484 (s), 1434 (s), 1414 (m), 1301 (w), 1265 (m), 1240 (m), 1174 (s), 1100 (m), 1040 (w), 950 (m), 941 (m), 869 (m), 819 (m), 763 (s), 752 (s), 708 (m), 619 (s, broad), 565 (m), 507 (w), 474 (m), 406 (m) cm^{-1}. MS (EI, 70 eV, 280 °C inlet): m/z (%) = 438 (70) [M^+], 409 (60) [$M^+ - N_2H$], 380 (80) [$M^+ - 2N_2H$], 354 (10), 305 (10), 294 (20), 205 (20), 191 (50), 190 (100), 176 (20), 163 (30), 150 (5). Raman IR: $\tilde{\nu}$ = 3259 (w) (N–H), 3065 (w) (C–H), 2218 (s) (C≡C), 1589 (m), 1468 (m), 1411 (m), 1146 (w).

[Co((tolaneN$_3$)$_2$)(py)$_2$] (3): Cobalt acetate tetrahydrate (56 mg, 0.25 mmol) and **2** (75 mg, 0.17 mmol) were dissolved in 3 mL of pyridine under slight warming to 50 °C in a water bath. The clear, dark red solution was left standing still at ambient temperature. After three days dark red crystals (75 mg, 54% of theory) had deposited. The crystals contain two molecules of pyridine per formula unit as solvate, which is easily given off. After some minutes in vacuo the crystals become opaque and disintegrate to a red powder. **3**·2py: $C_{38}H_{26}CoN_8$: calcd. C 69.8, H 4.0, N 17.1. For **3**: $C_{28}H_{16}CoN_6$: calcd. C 67.9, H 3.3, N 17.0; for **3**·2H$_2$O: $C_{28}H_{20}CoN_6O_2$: calcd. C 63.3, H 3.8, N 15.8; found C 65.7, H 4.6, N 15.1. IR (KBr): $\tilde{\nu}$ = 3061 (m), 3050 (w) (C–H), 2223 (w) (C≡C), 1601 (s), 1582 (s), 1563 (m), 1488 (s), 1466 (s), 1444 (s), 1436 (s), 1360 (w), 1311 (s), 1287 (s, broad), 1259 (s), 1209 (s), 1157 (m), 1140 (s), 1070 (m), 1039 (m), 1012 (w), 942 (s), 863 (w), 827 (m), 749 (s, broad), 719 (m), 692 (s), 646 (s), 632 (m), 566 (w), 479 (w), 458 (m), 430 (m) cm^{-1}. MS (ESI-ToF, positive): m/z = 991.16 ([Co((tolaneN$_3$)$_2$)]$_2$H$^+$), 536.1 ([Co((tolaneN$_3$)$_2$)]Na·H$_2$O$^+$), 496 ([Co((tolaneN$_3$)$_2$)]H$^+$), 440.1 ([Co((tolaneN$_3$)$_2$)]H$^+$ – 2N$_2$).

[Ni((tolaneN$_3$)$_2$)(py)$_2$] (4): Analogous to the preparation of **3**, nickel acetate tetrahydrate (56 mg, 0.25 mmol) and **2** (75 mg, 0.17 mmol) were dissolved in 3 mL of pyridine. After three days dark red crystals (40 mg, 54% of theory) deposited. The crystals were dried in vacuo giving a red powder. **4**·2py: $C_{38}H_{26}N_8Ni$: calcd. C 69.9, H 4.0, N 17.2; for **4**: $C_{28}H_{16}N_8Ni$: calcd. C 67.9, H 3.3, N 17.0; for **4**·2H$_2$O: $C_{28}H_{20}N_6NiO_2$: calcd. C 63.3, H 3.8, N 15.8; found C 68.0, H 4.3, N 16.6. MS (ESI-TOF, positive): m/z = 517.1 ([Ni((tolaneN$_3$)$_2$)]$_2$Na·H$_2$O$^+$), 495.1 ([Ni((tolaneN$_3$)$_2$)]$_2$H$^+$), 467.1 ([Ni((tolaneN$_3$)$_2$)]$_2$H$^+$ – N$_2$), 439.1 ([Ni((tolaneN$_3$)$_2$)]$_2$H$^+$ – 2N$_2$).

Crystal Structure Determinations: Data sets were recorded at ambient temperature with a Nonius CAD4 diffractometer using Cu-K_α radiation for **4**·2py and a Nonius kappa-CCD diffractometer using Mo-K_α radiation for **2** and **3**·2py. Crystal systems and space groups were unequivocally derived from the data sets and reciprocal space images. Analytical absorption corrections were applied to the data sets of **3**·2py and **4**·2py. The crystal structures were solved by Direct Methods[20] and refined against F^2 based on full-matrix least-squares with anisotropic displacement factors for all non-H atoms.[21] The H atoms in the structure of **2** were identified in difference fourier maps and refined as individual atoms with isotropic displacement parameters. H(1) and H(3) were refined as disordered with occupation factors of each 0.5. The H atoms in the structures of **3**·2py and **4**·2py were introduced in geometrically idealized positions and refined as riding on their respective C atoms with B_{iso} = 1.2 B_{eq} of the respective carbon atoms. Table 1 contains the crystallographic data and details of data collections and refinements, Table 2 selected bond lengths and angles. Graphical representations were drawn with the program Diamond.[22]

Table 1. Crystal data and details of data collection and refinement of **2**, **3**·2py, and **4**·2py.

Compound	(tolaneN$_3$H)$_2$ (**2**)	[Co((tolaneN$_3$)$_2$)(py)$_2$]·2py (**3**·2py)	[Ni((tolaneN$_3$)$_2$)(py)$_2$]·2py (**4**·2py)
Chemical formula	$C_{28}H_{18}N_6$	$C_{48}H_{36}CoN_{10}$	$C_{48}H_{36}NiN_{10}$
M [g mol^{-1}]	438.50	811.8	811.56
Crystal system	monoclinic	monoclinic	monoclinic
Space group	$P2_1/n$	$C2/c$	$C2/c$
a [Å]	6.0947(4)	23.7253(18)	23.618(4)
b [Å]	9.5435(9)	16.5533(9)	16.404(3)
c [Å]	18.5210(13)	10.8757(9)	10.817(2)
β [°]	95.098(5)	110.935(8)	110.64(2)
V [Å^3]	1073.01(14)	3989.3(5)	3921.9(12)
Z	2	4	4
$D_{calcd.}$ [g cm^{-3}]	1.357	1.352	1.375
μ [mm^{-1}]	0.08 (Mo-K_α)	0.48 (Mo-K_α)	1.10 (Cu-K_α)
F(000)	456	1684	1688
T [K]	293	293	293
Reflections collected	3746	72615	5445
Independent reflections	1889	4551	2507
Observed reflections with $I>4\sigma(F)$	976	3472	1548
R_{int}	0.067	0.078	0.042
Parameters refined	195	269	268
$R(\lvert F\rvert)$ for reflections with $I>4\sigma(F)$	0.050	0.050	0.056
$wR(F^2)$	0.119	0.1168	0.126
S	1.013	1.157	0.982
$\Delta\rho_{min}$ [eÅ^{-3}]	+0.15	+0.33	+0.22
$\Delta\rho_{max}$ [eÅ^{-3}]	–0.15	–0.33	–0.27

Table 2. Selected distances and angles in the structures of **2** and **3**·2py.

$(tolaneN_3H)_2$ **2** Distances [Å]			
C(1)–C(2)	1.197(3)	C(1)–C(22)	1.433(4)
N(1)–N(2)	1.299(3)	$C(2^{I})$–C(12)	1.434(4)
N(2)–N(3)	1.299(3)	phenyl ring 1	1.379(4) to 1.395(3)
N(1)–C(11)	1.418(3)	phenyl ring 2	1.374(4) to 1.396(3)
N(3)–C(21)	1.414(3)		
Angles [°]			
C(11)–N(1)–N(2)	113.5(2)	C(2)–C(1)–C(22)	179.0(3)
N(1)–N(2)–N(3)	114.2(2)	$C(1^{I})$–$C(2^{I})$–C(12)	178.7(3)
N(2)–N(3)–C(21)	115.1(2)	phenyl ring 1	119.2(2) to 120.6(3)
		phenyl ring 2	118.9(2) to 120.7(3)
$[Co((tolaneN_3)_2)(py)_2]$·2py (**3**·2py) Distances [Å]			
Co–N(1)	2.2092(17)	C(1)–C(2)	1.197(3)
Co–N(3)	2.2150(18)	C(1)–C(22)	1.435(3)
Co–N(4)	2.1447(19)	N(1)–C(11)	1.418(3)
N(1)–N(2)	1.315(2)	N(3)–C(21)	1.423(3)
N(2)–N(3)	1.311(2)	C(1)–C(22)	1.435(3)
		$C(2^{I})$–C(12)	1.425(3)
Angles [°]			
N(1)–Co–N(3)	58.06(6)	N(1)–N(2)–N(3)	109.70(17)
N(1)–Co–$N(3^{I})$	121.94(6)	N(2)–N(3)–C(21)	112.11(17)
C(11)–N(1)–N(2)	112.07(17)	C(2)–C(1)–C(22)	178.5(3)
		$C(1^{I})$–$C(2^{I})$–C(12)	177.8(2)

CCDC-716477 (for **2**), -716478 (for **3**·2py) and -716479 (for **4**·2py) contain the supplementary crystallographic data for this paper. These data can be obtained free of charge from The Cambridge Crystallographic Data Centre via www.ccdc.cam.ac.uk/data_request/cif.

Magnetic Measurements: The magnetic susceptibilities of **3** and **4** were determined on 3.4160 mg and 5.3989 mg samples in the temperature interval between 30 and 300 K using a Faraday balance. The sample of **3** was placed in an open quartz container and exposed to the vacuum. The weight decrease after evacuation showed that two equivalents of toluene per formula unit were evaporated. The sample of **4** was placed in a quartz container which was closed by flame-sealing. For **4**, a molecular mass according to the formula **4**·2py was assumed. Data points were taken every 10 K and 8 different field gradients were applied at each temperature point. A diamagnetic correction was applied to the observed weight data according to the method of atom and group increments.[23] The overall applied correction for **3** amounts to $-\chi_{dia} = 371.5 \times 10^{-6}\,cm^3\,mol^{-1}$ and $417.6 \times 10^{-6}\,cm^3\,mol^{-1}$ for **4**·2py. For the Ni-containing complex, in the region above 220 K some inconsistencies in the suszeptibilities at the different applied field gradients were observed, visible in Figure 6. These fluctuations may be caused by the small weight differences occurring at higher temperatures and the small magnetic moment of the Ni^{II} ions and are not caused by a significant field dependence.

Acknowledgments

We gratefully acknowledge the financial support of this work by the Deutsche Forschungsgemeinschaft (DFG) (within the Collaborative Research Area SFB 624) and CNPq/Brazil (research grant, proc. 309008/2006-9). Thanks are also due to J. Daniels for the collection of X-ray data and to N. Wagner for the susceptibility measurements.

---

[1] F. Marchesi, M. Turriziani, G. Tortorelli, G. Avvisati, F. Torino, L. De Vecchis, *Pharmacol. Res.* **2007**, *56*, 275–287.
[2] D. B. Kimball, M. M. Haley, *Angew. Chem. Int. Ed.* **2002**, *41*, 3338–3351.
[3] D. B. Kimball, R. Herges, M. M. Haley, *J. Am. Chem. Soc.* **2002**, *124*, 1572–1573.
[4] P. Gantzel, R. J. Walsh, *Inorg. Chem.* **1998**, *37*, 3450–3451.
[5] H. S. Lee, S.-O. Hauber, D. Vinduš, M. Niemeyer, *Inorg. Chem.* **2008**, *47*, 4401–4412.
[6] A. G. M. Barrett, M. K. Crimmin, M. S. Hill, P. B. Hitchcock, G. Kociok-Köhn, P. A. Procopiu, *Inorg. Chem.* **2008**, *47*, 7366–7376.
[7] I. A. Guzei, L. M. Liable-Sands, A. L. Rheingold, C. H. Winter, *Polyhedron* **1997**, *16*, 4017–4022.
[8] M. Hörner, G. M. de Oliveira, A. J. Bortoluzzi, *Z. Anorg. Allg. Chem.* **2006**, *632*, 537–539.
[9] J. Ruiz, J. F. J. López, V. Rodríguez, J. Pérez, M. C. R. de Arellano, G. López, *J. Chem. Soc., Dalton Trans.* **2001**, 2683–2689.
[10] a) S. F. Gait, M. E. Peek, C. W. Rees, R. C. Storr, *J. Chem. Soc., Chem. Commun.* **1972**, 982–983; b) S. F. Gait, M. E. Peek, C. W. Rees, R. C. Storr, *J. Chem. Soc. Perkin Trans. 1* **1974**, 1248–1260.
[11] a) M. Hörner, G. M. de Oliveira, J. S. de Oliveira, W. M. Teles, C. A. L. Filgueiras, J. Beck, *J. Organomet. Chem.* **2006**, *691*, 251–254; b) M. Hörner, A. J. Bortoluzzi, J. Beck, M. Serafin, *Z. Anorg. Allg. Chem.* **2002**, *628*, 1104–1107.
[12] A. Kliegl, *Ber. Dtsch. Chem. Ges.* **1908**, *40*, 4937–4941.
[13] A. Kliegl, K. Haas, *Ber. Dtsch. Chem. Ges.* **1911**, *44*, 1209–1218.
[14] P. Knops, F. Vögtle, *Chem. Ber.* **1991**, *124*, 1223–1227.
[15] Cambridge Structural Database CSD, The Cambridge Crystallographic Data Centre, Cambridge, UK, Release 5.29, November **2007**.
[16] S.-M. Peng, Y.-N. Lin, Y. Wang, *Bull. Inst. Chem. Acad. Sin.* **1985**, *32*, 1.
[17] V. V. Sushchev, A. N. Kornev, Yu. A. Kurskii, O. V. Kuznetsova, G. K. Fukiu, G. A. Abakumov, *Russ. Chem. Bull.* **2005**, *114*, 1585.
[18] H. Lueken, *Magnetochemie*, Teubner Publishers, Stuttgart, Germany, **1999**.
[19] K.-J. Chang, D. Moon, M. S. Lah, K.-S. Jeong, *Angew. Chem. Int. Ed.* **2005**, *44*, 7926–7929.
[20] G. M. Sheldrick, *SHELXS-93*, *Program for crystal structure solution*, University of Göttingen, Germany, **1993**.
[21] G. M. Sheldrick, *SHELXL-97*. *Program for crystal structure refinement*. University of Göttingen, Germany, **1997**.
[22] *Diamond, Program for Crystal and Molecular Structure Visualization*, Crystal Impact GbR., Bonn, Germany, **2008**.
[23] A. Weiss, H. Witte, *Magnetochemie*, Verlag Chemie, Weinheim, Germany, **1973**.

Received: May 23, 2009